International Journal of Pharmaceutical Drug Design
IJPDD (February, 2025)
ISSN: 2584-2897
Website: https://ijpdd.org/

DOI: 10.62896/ijpdd.2.2.2
Research

Biocompatible Thermoresponsive Gels Enriched with Rosemary Essential Oil for Advanced Antimicrobial and Drug Delivery Applications

Nitin Dahiya[1], Soumik Chatterjee[2], Sriparna Chakraborty[3], Dr. Atika Ismail[4], M. Jasvitha[5], Shivangi Sharma*[6]

[1]*Assistant Professor, Starex University, Gurugram 122413*
[2]*Post Graduate Resident, KPC Medical College & Hospital, Jadavpur, Kolkata 700032*
[3]*Research Scholar, University of Calcutta, 92, A.P.C. Road, Kolkata 700009*
[4]*Doctor, Consultant Periodontist*
[5]*Student, Vignan Institute of Pharmaceutical Technology, Besides VSEZ, Duvvada,Vadlapudi Post , Gajuwaka Visakhaptnam -530049, India.*
[6]*Scholar, Lovely Professional University, Jalandhar, 144411*

Received: *05-12-2024* / ***Revised:*** *23-01-2025* / ***Accepted:*** *10-02-2025*
Corresponding Author: *Adarsh Kumar*
Email: *shivisharma125@gmail.com*
Conflict of interest: *Nil*

Abstract:

This work explores the creation of biocompatible thermoresponsive gels that are enhanced with poly(lactic-co-glycolic) acid (PLGA) microparticles containing rosemary essential oil (RoEO). The goal is to improve drug delivery systems and antibacterial capabilities. A solution to the problems caused by essential oil volatility and degradation was found by incorporating RoEO, a naturally occurring bioactive chemical with strong antibacterial and antioxidant capabilities, inside PLGA microparticles. This allowed for its controlled release. Topical medication administration is useful for wound healing and infection treatment due to the thermoresponsive nature of the gel formulations, which allow in situ gelation at physiological temperatures. The RoEO-PLGA gels were tested for their antimicrobial properties against several microorganisms, including Staphylococcus aureus, Escherichia coli, and Candida albicans. Most notably, they demonstrated significant inhibition against C. albicans, suggesting that they might have antifungal uses. The formulations were determined to be stable and suitable for use as controlled release systems by rheological and thermal tests. Integrating the medicinal potential of essential oils with biodegradable polymers, the work offers a viable method to building effective and patient-friendly drug delivery platforms. Evaluating the efficacy of these systems in in vivo models and improving their clinical performance should be the primary goals of future research.

Keywords: Biocompatible gels, Rosemary essential oil (RoEO), Poly(lactic-co-glycolic) acid (PLGA), Thermoresponsive systems, Antimicrobial properties, Drug delivery systems

1. Introduction

Biomedical researchers have recently focused on ways to create more effective drug delivery systems by combining biocompatible materials with thermoresponsive properties. Among the many benefits of thermoresponsive gels—which may change their phase from liquid to solid in reaction to variations in temperature—are their controlled release, low toxicity, and simplicity of application. Particularly promising for several medicinal uses, including drug administration, tissue engineering, and wound healing, are thermoresponsive gels made of polymers like Poloxamers, which can gel at physiological temperatures. The therapeutic efficiency of these systems might be enhanced by the inclusion of bioactive chemicals, such as essential oils, which could have functional and medical advantages. (1) and (2). Medicinal plant essential oils (EOs) are one kind of natural substance that has gained attention for its powerful antibacterial, antioxidant, and anti-inflammatory capabilities. One plant that has attracted interest is Rosmarinus officinalis, or rosemary, because of its rich chemical makeup. This composition is mostly made up of monoterpenes, which have strong antioxidant and

antibacterial effects [3][4]. In regions where antibacterial activity and controlled drug release are crucial, the therapeutic effectiveness of biomedical formulations might be enhanced by using rosemary essential oil (RoEO) [5][6].

An successful technique for regulated medication delivery has recently been investigated, and it involves combining essential oils with biodegradable polymers like Poly(D,L-lactide-co-glycolide) acid (PLGA) [7][8]. Because of its versatility in encapsulating active substances and facilitating their regulated release over long periods of time, PLGA—a biocompatible and biodegradable polymer—has seen considerable usage in drug delivery systems. Essential oils, such as RoEO, may be controlled-released when encapsulated in PLGA-based matrices, which increases the active components' stability and guarantees their therapeutic benefits last. The quick deterioration and extreme volatility of essential oils are two problems that this method may help solve [9]. To further enhance the bioavailability of these active chemicals, a novel approach might be taken via the creation of thermoresponsive PLGA-based gels. Transdermal medication administration, wound healing, and other topical therapies may be achieved using formulations that react to physiological temperature fluctuations. These formulations can undergo in situ gelation upon skin application. The antibacterial characteristics of these thermoresponsive systems might be improved with the addition of rosemary essential oil, making them useful for the treatment of infections, especially in skin lesions or wounds [10][11]. This work explores the creation of thermoresponsive gels that include PLGA microparticles loaded with rosemary essential oil. The goal is to create a platform that can deliver drugs in a regulated manner and also kill microbes. In order to optimise the formulation of these gels for prospective therapeutic applications in improved drug delivery and antimicrobial therapies, this study undergoes a variety of characterisations, including chemical, physical, and antimicrobial testing [12][13].

2. Materials and Methods

2.1 Plant Material and Essential Oil Extraction

In August 2024, the leaves of the Rosmarinus officinalis plant were collected from the southwest Indian botanical garden. A herbarium at the Pharmaceutical Botany Department of the Faculty of Pharmacy at the University of Medicine and Pharmacy of [Institution Name] in India received the plant specimens. Excluded from the study were any species that are currently protected or in risk of extinction. Items were meticulously cleaned, then left to air-dry in cool, shaded areas until they were ready to be ground for extraction. One hundred grammes of dried and powdered leaves were hydro-distilled for four hours in a round-bottom flask with one thousand millilitres of distilled water using a system similar to the NeoClevenger. After passing the mixture through a condenser, the rosemary essential oil (RoEO) was collected in a graduated column after it had been heated. After the RoEO was hydro-distilled, it was transferred to glass vials, dehydrated with anhydrous sodium, and stored at 4°C in opaque, tightly sealed containers for further analysis.

2.2 Chemicals and Reagents

has a molecular weight range from 40,000 to 75,000, together with 65% poly(D,L-lactide-co-glycolide) acid, 35% poloxamer, and 8% RoEO in a dichloromethane (DCM) solution, 8% PVA (8-88), and 7% filtered water.

2.3 GC–MS Analysis

The purpose of this investigation was to determine RoEO's chemical composition. In order to understand its potential antibacterial properties—that serve as the foundation of our formulations—it was crucial to identify the main components. In order to determine the chemical composition of RoEO, a thorough study was carried out using GC-MS. In this method, reference spectra from the NIST Library (2020 edition) were compared to the target samples, allowing for the identification and quantification of individual elements. Integrating an AI/AS 3000 autosampler and DSQ II mass spectrometer, the analytical setup made use of a Thermo Scientific Focus GC equipment (Noida, India). For chromatographic separation, a TraceGOLD TG-624 capillary column was used. The column was 60 meters in length, with an inner diameter of 0.25 millimetres, and a film thickness of 1.4 micrometres. A volume of 1 µL was used for injecting samples, with helium serving as the carrier gas and a flow rate of 1.4 mL/min. We used a division injection approach with a ratio of 1:50. The GC oven was preheated to 90°C and then increased at a rate of 3°C per minute until it reached 220°C; this temperature was maintained at 220°C for five minutes to ensure perfect separation. In order to guarantee accurate detection, the mass spectrometry settings were fine-tuned. We set the transfer line temperature to 240 °C and the ion source temperature at 230 °C. A 70 eV energy threshold was used for electron impact ionisation (EI). The data was acquired using a mass-to-charge (m/z) spectrum ranging from 50 to 450, using comprehensive scan mode. To ensure uniformity, every examination was repeated three times. We measured and accurately identified the components by recording their retention periods and comparing their mass spectra to those in the NIST Library Reference Database. An in-depth examination of RoEO was made possible by this thorough GC-MS technology, which provided significant disclosures about its chemical composition.

2.4 Preparation of RoEO-PLGA Microparticles

Using the oil-water emulsion process, RoEO-PLGA microparticles were synthesised. First, 1 millilitre of RoEO (either extracted or from the reference) was mixed with 5 millilitres of PLGA solution (500 mg dissolved in 5 millilitres of DCM) and then vortexed at 40,000 rpm in a SilentCrusher. Over the course of five hours, the organic solvent was progressively evaporated by slowly adding the oil phase to a water solution that already contained 0.5% PVA while being constantly stirred at 900 rpm. After collecting the particles, they were centrifuged at 11,000 rpm in an Eppendorf 5804 before being washed extensively. This was followed by lyophilization using Alpha

1-2 LSCbasic freeze drier. The process required overnight freezing of the particles in suspension at 55°C and continuous maintenance of a vacuum of 0.02 mbar for 48 hours. For future studies, the RoEO-PLGA microparticles were kept in the fridge.

2.5 Gel Formulation

We opted to evaluate the lowest and highest concentrations of the two poloxamers (Poloxamer 407 and Poloxamer 188) as a first benchmark to study the feasibility and effectiveness of thermoresponsive gel formulations that include RoEO-loaded PLGA nanoparticles. This technique not only laid the framework for understanding how these variables affected the gel's performance, but it also allowed us to evaluate the differences in critical aspects such as pH levels, viscosity, and rheological features. After preparing 150 mg of RoEO-PLGA in 4°C cold water, over 100 mL of the aqueous solution was added to a magnetic Raypa plate set in an ice bath and stirred. Two formulations were used for this purpose: (A) a 25% (w/v) Poloxamer 407/polymer 188 combination, or (B) a 20% (w/v) Poloxamer 407/polymer 188 mixture. Both the RoEO-PLGA _A and RoEO-PLGA _B formulations were the end results.

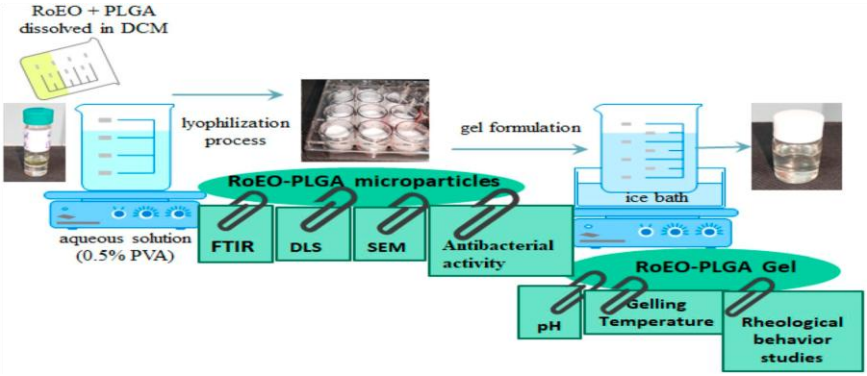

Figure 1. Graphic process of RoEO-PLGA microparticles and RoEO-PLGA gels formulation and characterization. DCM: Dichloromethane; DLS: Dynamic light scattering; FTIR: Fourier-transform infrared; PLGA: Poly(lactic-co-glycolic) acid; PVA: Poly(vinyl alcohol); RoEO: Rosemary essential oil; SEM: Scanning electron microscopy.

2.6 FTIR Spectroscopy

The lyophilised RoEO-PLGA microparticles sample was used to conduct FTIR measurements on a solid-state specimen. This ensured that the results accurately reflected the actual molecular composition and interactions within the formulation. The spectrometer used was a Shimadzu AIM-9000 with attenuated total reflectance (ATR) accessories from Shimadzu in Bangalore, India. In the range of 4000 to 400 cm−1, the spectra were recorded using 20 scans, resulting in a 4 cm−1 resolution. Thoroughly reviewing relevant academic literature allowed for the establishment of wavelength allocation.

2.7 XRD Analysis

The X-ray diffraction analysis was conducted using a Bruker AXS D8-Advance diffractometer (Bruker AXS Pvt. Ltd., New Delhi, India), employing CuKα radiation (λ = 0.1541 nm). The apparatus boasts a dynamic sample platform and incorporates an Anton Paar TTK low-temperature chamber, proficient in functioning within a range of −180°C to 450°C. Additionally, it includes a high-temperature chamber designed to handle temperatures soaring up to 1600°C. Furthermore, the device upholds elevated vacuum states, a non-reactive environment, and regulation of moisture levels. The ensuing XRD patterns were meticulously analysed in relation to the ICDD Powder Diffraction Database.

2.8 SEM Analysis

High-resolution SEM images were obtained utilising a JSM-IT200 InTouchScope™ Scanning Electron Microscope (Bengaluru, India), featuring a field emission gun (FEG) alongside an energy-dispersive X-ray spectroscopy (EDS) apparatus.

2.9 DLS Particle Size Distribution Analysis

The DLS examination was performed utilising a Microtrac/Nanotrac 252 device located in Pune, India. Every specimen underwent measurement in triplicate at room temperature (22°C) and at a scattering angle of 172 degrees.

2.10 Thermal Analysis

A thermal evaluation was performed to examine the thermal resilience and breakdown characteristics of the formulations. This was crucial for validating that the encapsulated RoEO and the PLGA matrix maintain their stability during both storage and application scenarios. A thermal examination was performed utilising an aluminium crucible on the TGA/DSC 3+ (Mettler-Toledo India), which is outfitted with a digital temperature sensor and an analogue differential thermal analysis (DTA) sensor. The evaluations were conducted within a vibrant air environment, characterised by oxidative circumstances utilising synthetic air at a flow rate of 20 mL/min, spanning temperatures from 25 to 400°C, with a heating increment of 10°C/min.

2.11 pH Measurement

The acidity levels of the gels were assessed using an HI991003 pH meter from Hanna Instruments (Mumbai, India).

2.12 Viscosity and Rheological Behavior Studies

Viscosity and rheological behavior studies examined the mechanical and flow properties of the gels. The rheological properties of the two formulations were analyzed using a rotational viscometer (HAAKE Viscotester 550; Thermo Scientific, Noida, India) equipped with Lauda immersion thermostat A 100 and water bath 006T. Viscosity was determined at different temperatures, and at rotational speeds ranging from 3 to 600 rpm. The gelation temperature was recorded as the temperature was raised from 25 to 40°C at a heating rate of 1°C/min.

2.13 Assessment of the Antimicrobial Properties

Using the agar diffusion method, the antimicrobial activity of RoEO was further evaluated against standard bacterial strains (*S. aureus* ATCC 29213 and *E. coli* ATCC 25922) and one fungal standard strain (*C. albicans* ATCC 14053). The inoculums with 0.5 turbidity on a McFarland scale of the above-named standardized strains were applied on a Müller–Hinton agar within 15 min of preparation. Blank antimicrobial susceptibility paper disks with a 6 mm diameter (Thermo Scientific, India) were carefully infused with the test samples. These samples were carefully handled using sterilized forceps and were subsequently placed on the surface of Müller–Hinton agar plates. As a negative control, a paper disc infused with water was used. The Petri dishes were afterwards incubated at 37°C for 24 hours. The antimicrobial activity of the tested samples was established through the measurement of the total inhibition diameters of the bacterial and fungal growth, respectively, including the disk area. The diameter of inhibition zones was expressed in mm.

2.14 Statistical Analysis

All experiments were performed in triplicate for all samples, all calibration curves, and concentrations. Statistical analysis was carried out using Microsoft Office Excel and expressed as mean ± standard deviation (SD). p-values < 0.05 were considered statistically significant. Graphical figures were obtained with ConceptDraw Diagram software (version 18).

3. Results and Discussion

3.1 GC–MS Analysis

The antibacterial activity of RoEO is greatly influenced by the composition's dominance of monoterpenes, which include both hydrocarbons and oxygenated versions (refer to Table 1; see Figures 2 and 3). This was shown via the study using GC-MS. With an increased concentration of oxygenated monoterpenes, the antibacterial efficacy is much enhanced (58.7% in RoEO vs to 68.46% in the RoEO Tunisia reference).

Table 1. Compounds identified in rosemary essential oil.

No.	Compound	tR (min)	RI (NIST)	RoEO	RoEO Tunisia Reference
1.	tricyclene	6.56	933	0.36	0.11
2.	camphene	7.59	950	9.76	3.27
3.	2,4-thujadiene	7.73	971	0.18	0.03
4.	β-pinene	8.73	972	0.34	5.33
5.	α-pinene	8.74	939	17.4	11.11
6.	1-octen-3-ol	8.82	1078	0.14	0.02
7.	3-octanone	9.07	1121	0.2	0.03
8.	α-myrcene	9.27	991	2.87	0.86
9.	β-thujene	9.36	964	–	0.23
10.	3-octanol	9.61	1126	–	–
11.	α-phellandrene	10.04	1015	0.16	0.11
12.	3-carene	10.14	1030	0.03	0.11
13.	α-terpinene	10.56	1016	0.63	0.36
14.	β-cymene	10.95	1018	2.02	1.57
15.	D-limonene	11.19	1031	3.59	1.86
16.	eucalyptol	11.35	1034	14.29	52.77
17.	β-cis-ocimene	12.12	1049	–	0.03
18.	γ-terpinene	12.72	1062	0.62	0.6
19.	linalool	15.15	1095	0.77	0.57
20.	crysanthenone	16.31	1102	0.08	–
21.	terpinolene	17.47	1088	0.38	0.26
22.	camphor	17.9	1146	29.69	9.27
23.	camphenilanol	18.31	1151	–	–
24.	sabinone	18.76	1162	0.05	–
25.	pinocarvone	18.76	1191	–	–
26.	D-pinocamphone	18.85	1206	0.09	0.02

27.	endo-borneol	19.4	1163	4.7	2.6
28.	terpinen-4-ol	19.95	1176	0.59	0.58
29.	α-terpinyl propionate	20.91	1333	1.58	1.78
30.	verbenone	21.56	1204	3.19	0.04
31.	trans-shisool	23.76	1326	–	–
32.	(+)-borneol acetate	25.45	1330	3.48	0.81
33.	(+)-cis-verbenol acetate	25.68	1351	–	0.01
34.	thymol	25.91	1290	0.07	–
35.	piperitenone	26.92	1303	0.05	–
36.	α-cubebene	27.61	1374	–	0.02
37.	ylangene	27.68	1395	0.06	0.05
38.	copaene	27.82	1415	0.04	0.22
39.	carvacrol	28.04	1298	0.05	–
40.	methyleugenol	28.34	1396	–	0.01
41.	caryophyllene	28.71	1420	1.47	3.77
42.	humulene	29.36	1454	–	0.38
43.	p-thymol	29.58	1465	–	–
44.	7-epi-α-cadinene	29.76	1491	0.04	0.02
45.	α-bisabolene	30.2	1506	–	0.05
46.	(-)-δ-cadinene	30.36	1520	0.11	0.23
47.	trans-calamenene	30.41	1542	0.02	–
48.	α-calacorene	30.72	1561	0.04	0.01
49.	(+)-sativen	30.94	1583	–	–
50.	cubenol	32.01	1600	–	–
51.	α-bisabolol	32.62	1621	0.01	0.01
52.	levomenthol	32.62	1632	0.02	–
53.	caryophyllene oxide	38.74	1652	0.02	0.1
	Total No. of compounds identified			38	38
	Total (%)			99.19	99.21
	Monoterpene hydrocarbons (%)			38.34	25.84
	Oxygenated monoterpenes (%)			58.7	68.46
	Sesquiterpene hydrocarbons (%)			1.78	4.75
	Oxygenated sesquiterpenes (%)			0.03	0.11
	Other compounds (%)			0.34	0.05

NIST: National Institute of Standards and Technology (USA); RI: Retention index; RoEO: Rosemary essential oil; tR: Retention time.

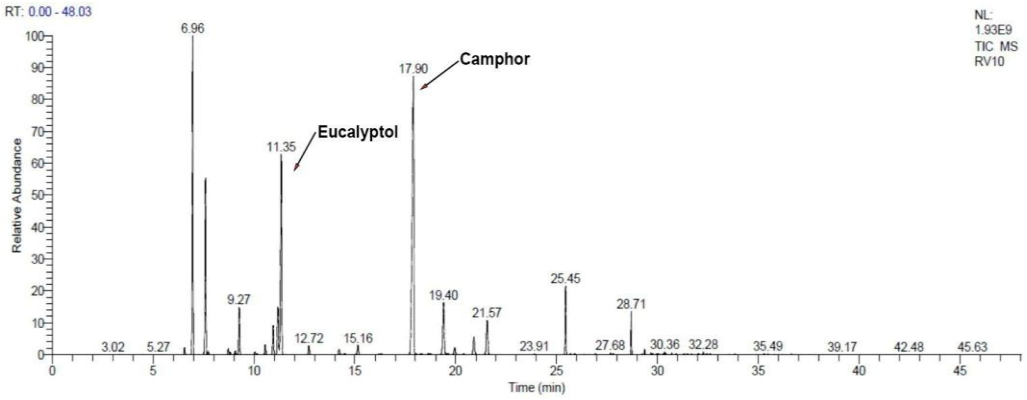

Figure 2. GC–MS chromatogram of RoEO Tunisia reference. GC: Gas chromatography; MS: Mass spectrometry; RoEO: Rosemary essential oil.

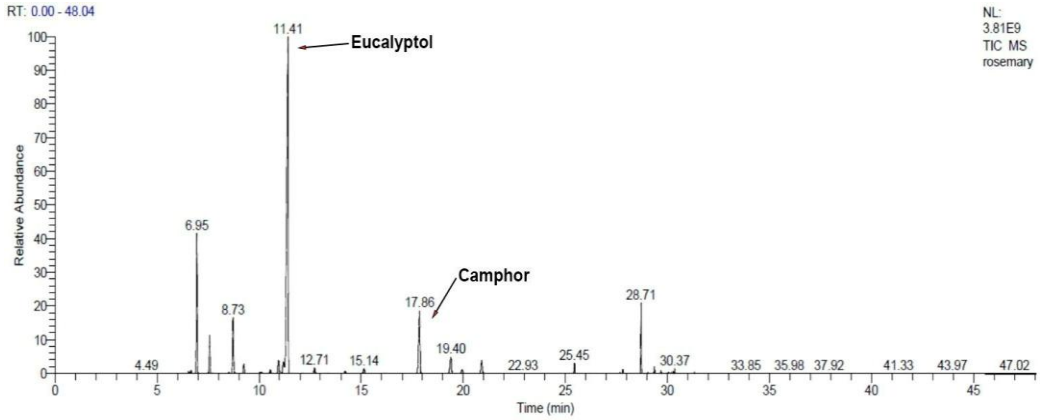

Figure 3. GC–MS chromatogram of RoEO sample.

3.2 FTIR Analysis

The FTIR spectra presented in Figure 4 provide valuable insights into the chemical characteristics of three substances: Poly(lactic-co-glycolic) acid (PLGA), Rosemary essential oil (RoEO), and the RoEO-PLGA composite formulation. The spectrum of PLGA reveals key peaks, including one at approximately 1754 cm−1, associated with the stretching vibrations of the ester carbonyl group, and another at 1180 cm−1, corresponding to the C–O–C ether bond. These peaks are characteristic of PLGA's polymeric structure and its ester-based functionality.

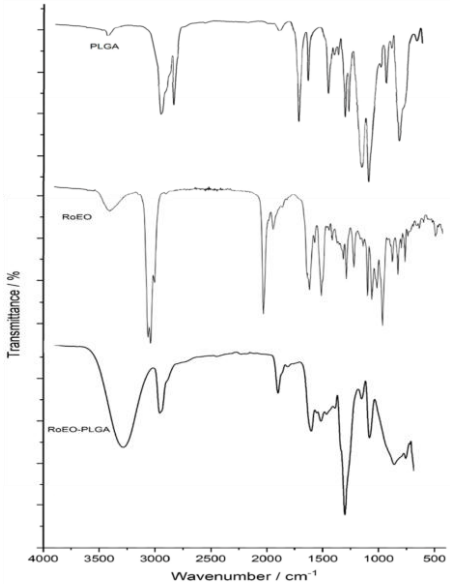

Figure 4. FTIR spectra for PLGA, RoEO, and RoEO-PLGA samples. FTIR: Fourier-transform infrared; PLGA: Poly(lactic-co-glycolic) acid; RoEO: Rosemary essential oil.

The RoEO spectrum, by contrast, showcases typical peaks of essential oils, particularly the broad O–H stretching band at 3434 cm−1 and the carbonyl (C=O) stretching around 1746 cm−1. These peaks are indicative of the hydroxyl and carbonyl functional groups present in the monoterpenes and other bioactive compounds that make up the rosemary oil. In the FTIR spectrum of the RoEO-PLGA formulation, the presence of overlapping peaks from both the PLGA and RoEO spectra validates the successful incorporation of rosemary oil into the polymeric matrix. Specifically, a broad band at 3305 cm−1 is attributed to O–H stretching vibrations, originating from both PLGA and RoEO, confirming the integration of the essential oil. The peak at 1758 cm−1 also reflects the ester bonds present in PLGA, suggesting strong interaction between the polymer and the encapsulated oil. These findings demonstrate that the encapsulation process preserves the functional integrity of the rosemary oil, which is crucial for maintaining its controlled release properties in therapeutic applications.

3.3 XRD Analysis

The X-ray diffraction (XRD) patterns presented in Figure 5 demonstrate the structural properties of three materials: Poly(lactic-co-glycolic) acid (PLGA), Rosemary essential oil (RoEO), and the RoEO-PLGA composite formulation. The PLGA sample shows a typical amorphous characteristic with a broad, shallow peak around 20° (2θ), indicative of its non-crystalline structure. This broad diffraction peak suggests that PLGA lacks well-defined crystalline regions, as is typical for many polymers, which is beneficial for its use in drug delivery systems, as amorphous materials tend to have better solubility and more controlled release properties.

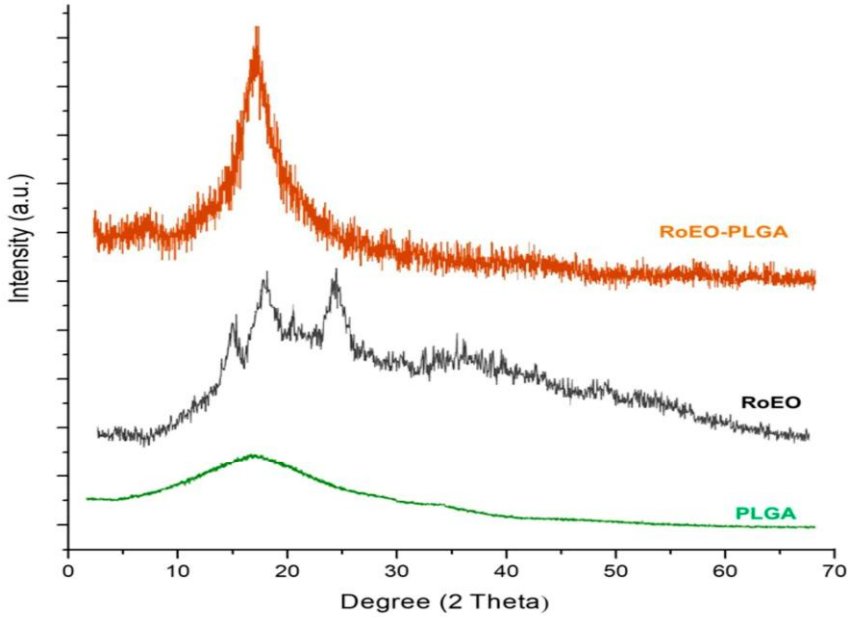

Figure 5. XRD pattern of PLGA, RoEO, and RoEO-PLGA samples. XRD: X-ray diffraction.

In contrast, the RoEO sample displays a sharper diffraction peak at a slightly higher 2θ value, around 20°, indicating that rosemary essential oil has a semi-crystalline or amorphous nature depending on its chemical composition. However, the RoEO-PLGA composite formulation (represented by the orange trace) shows a significant shift in the diffraction pattern, with a broader and less defined peak compared to pure RoEO, which aligns with the amorphous nature of PLGA. This change suggests that the rosemary essential oil has been effectively encapsulated within the PLGA matrix, preventing the formation of crystalline regions and preserving its amorphous characteristics. The absence of sharp diffraction peaks in the RoEO-PLGA formulation further confirms that the essential oil is successfully incorporated into the polymer, which is crucial for ensuring the controlled release of its bioactive compounds in therapeutic applications.

3.4 Morphological Studies

3.4.1 SEM Analysis

Figure 6 presents a scanning electron microscopy (SEM) image of the morphological characteristics of RoEO-PLGA microparticles. The image reveals that the microparticles exhibit a spherical shape with distinct, well-defined edges, indicating the successful formation of uniform particles. The surface of the microparticles appears relatively smooth with some degree of roughness, which may contribute to their stability and dispersibility in a gel formulation. The size distribution of the particles appears to be relatively consistent, with the particles clustered in groups, likely due to the drying process used before the SEM analysis. These structural features suggest that the microparticles are well-formed and suitable for encapsulating rosemary essential oil (RoEO) in drug delivery applications, ensuring that the bioactive compounds are efficiently encapsulated and released over time. The scale bar in the image indicates a particle size of approximately 20 µm, further highlighting the microstructural properties of the RoEO-PLGA formulation.

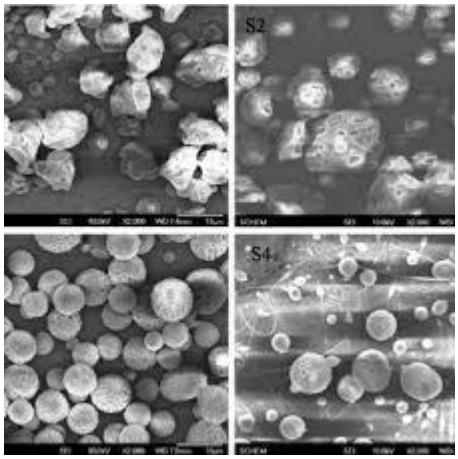

Figure 6. Morphological aspects of RoEO-PLGA microparticles (SEM image). SEM: Scanning electron microscopy.

3.4.2. EDS Spectrum

Figure 7 displays the Energy-Dispersive X-ray Spectroscopy (EDS) spectrum of the RoEO-PLGA microparticles, providing valuable insights into the elemental composition of the sample. The spectrum reveals several peaks corresponding to various elements, including carbon (C), oxygen (O), silicon (Si), calcium (Ca), magnesium (Mg), aluminum (Al), and chlorine (Cl). These elements are

primarily associated with the PLGA polymer matrix and the encapsulated rosemary essential oil (RoEO). The strong peaks for carbon (C) and oxygen (O) reflect the organic nature of the materials, particularly the polymer backbone of PLGA and the chemical composition of the essential oil. The presence of elements such as calcium (Ca) and magnesium (Mg) may indicate trace minerals that are naturally present in the rosemary essential oil or result from the formulation process. This elemental analysis confirms the successful incorporation of RoEO into the PLGA matrix, highlighting the stability and integrity of the encapsulated system, which is crucial for its application in controlled drug delivery and antimicrobial treatments.

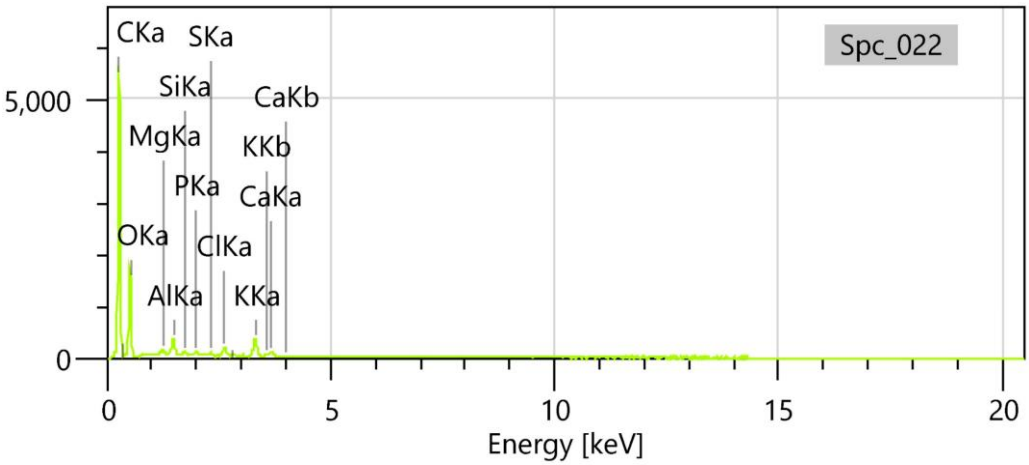

Figure 7. EDS spectrum of RoEO-PLGA microparticles. EDS: Energy-dispersive X-ray spectroscopy.

3.4.3. DLS Analysis

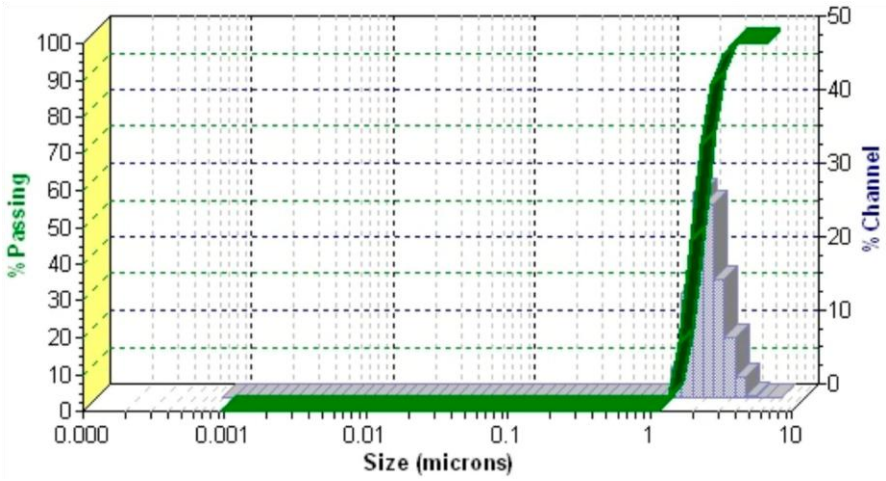

Figure 8. DLS pattern of RoEO-PLGA sample.

Figure 8 presents the Dynamic Light Scattering (DLS) pattern for the RoEO-PLGA sample, which is used to determine the size distribution of the microparticles within the formulation. The graph shows a sharp increase in the percentage of particles passing through the channels as the particle size approaches 1 micron. The majority of the particles in the RoEO-PLGA sample are below 1 micron in size, which is ideal for efficient drug delivery, as smaller particles can better disperse and penetrate biological barriers. The histogram in the lower part of the graph further confirms the uniform distribution of particle sizes, with a significant concentration of particles in the sub-micron range. This DLS analysis is essential for evaluating the quality and consistency of the microparticles in the formulation, as uniform particle sizes ensure predictable release profiles and enhance the stability of the encapsulated rosemary essential oil (RoEO) for its intended therapeutic and antimicrobial applications.

3.5 Thermal Analysis

Figure 9 illustrates the thermoanalytical data for the RoEO-PLGA sample, which provides insights into the thermal stability and behavior of the formulation. The graph features three distinct lines: the black line represents Thermogravimetric (TG) analysis, the green line represents Derivative Thermogravimetry (DTG) analysis, and the red line represents Heat Flow (HF). The TG analysis line reveals the percentage mass loss of the sample as a function of temperature, indicating the stages of decomposition. The most significant mass loss occurs at around 200°C, marking the initial phase of decomposition, which likely corresponds to the breakdown of volatile components, including the rosemary essential oil (RoEO). This initial loss aligns with the typical thermal degradation of the PLGA matrix, highlighting the volatility of essential oils when incorporated into polymeric matrices.

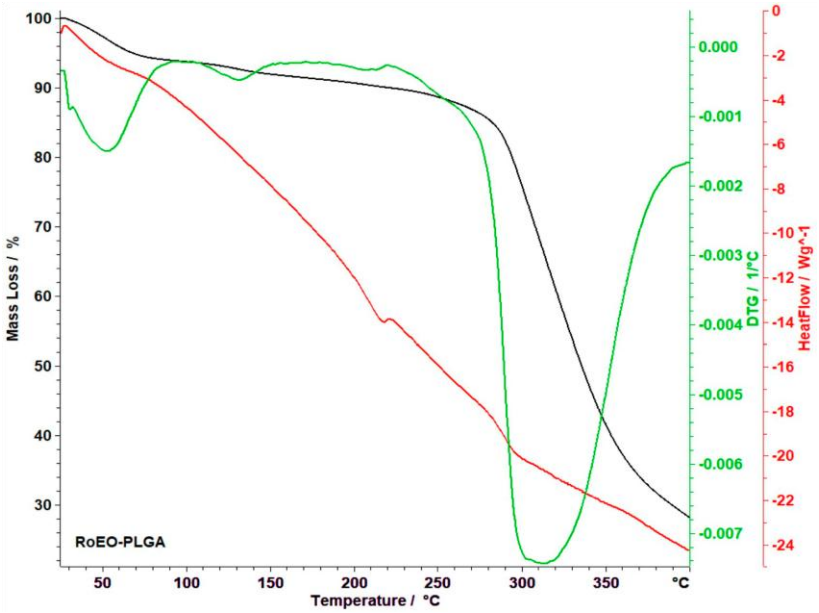

Figure 9. Thermoanalytical data for RoEO-PLGA sample (black line: TG analysis; green line: DTG analysis; red line: HF). DTG: Derivative thermogravimetry; HF: Heat flow; TG: Thermogravimetry.

The DTG curve, depicted by the green line, complements the TG data by providing the rate of mass loss with respect to temperature. The sharp peaks at around 200°C and 300°C suggest distinct stages of decomposition. The first peak at 200°C corresponds to the rapid loss of mass, associated with the loss of water and potentially low molecular weight components. The second peak, which appears at higher temperatures (~300°C), indicates the degradation of the PLGA polymer itself. This thermal decomposition is essential to understand, as it dictates the stability of the formulation under varying temperature conditions, which is crucial for drug delivery and long-term storage. The HF analysis, represented by the red line, shows the heat flow associated with the decomposition process. It reveals the endothermic and exothermic events occurring during the thermal analysis, such as the heat absorption associated with the release of moisture and solvents at lower temperatures and the heat evolution during the polymer's degradation at higher temperatures. The heat flow data, combined with TG and DTG analyses, provides a comprehensive understanding of the RoEO-PLGA system's thermal properties. These analyses suggest that while the formulation is thermally stable up to approximately 200°C, the polymer backbone begins to degrade at higher temperatures, which may influence the release of the encapsulated rosemary essential oil (RoEO). This detailed thermal behavior is vital for ensuring the formulation's stability during processing, storage, and application, especially for controlled drug release and antimicrobial treatments.

3.6 Gelation Temperature and pH

Table 2 presents the gelation temperature, pH, and gelation time for two different formulations of the RoEO-PLGA system, denoted as RoEO-PLGA _A and RoEO-PLGA _B. The gelation temperature refers to the temperature at which the formulation transitions from a liquid state to a gel state, an important characteristic for thermoresponsive gels. The data shows that RoEO-PLGA _A exhibits a gelation temperature of 27.6 ± 0.047°C, while RoEO-PLGA _B has a higher gelation temperature of 32.9 ± 0.094°C. This difference in gelation temperature indicates that the formulation with a higher concentration of Poloxamer 407 (RoEO-PLGA _B) requires a slightly higher temperature to undergo gelation, which could be beneficial for applications involving varying skin or body temperatures. The pH values of the two formulations are also presented, which are essential for skin compatibility. The pH of RoEO-PLGA _A is 6.63 ± 0.024, while RoEO-PLGA _B has a slightly lower pH of 6.40 ± 0.016. Both pH values fall within the ideal range for topical formulations, as they are close to the natural pH of the skin, ensuring minimal irritation and optimal compatibility for transdermal applications. Furthermore, the gelation time, which is the duration it takes for the formulation to form a gel at the designated gelation temperature, is 58 seconds for RoEO-PLGA _A and 45 seconds for RoEO-PLGA _B. The shorter gelation time for formulation _B indicates faster gel formation, which may be advantageous for quicker application and sustained release of the encapsulated active ingredients, including rosemary essential oil (RoEO), in clinical settings. This data underscores the potential of both formulations for use in targeted drug delivery, wound healing, and other biomedical applications.

Table 2. Gelation temperature, pH and gelation time of the two formulations (results expressed as mean ± SD).

Formulation	Gelation Temperature (◦C)	pH	Gelation Time (s)
RoEO-PLGA _A	27.6 ± 0.047	6.63 ± 0.024	58

RoEO-PLGA _B	32.9 ± 0.094	6.40 ± 0.016	45

PLGA: Poly(lactic-co-glycolic) acid; RoEO: Rosemary essential oil; SD: Standard deviation.

3.7 Viscosity and Rheological Behavior

RoEO-PLGA _A and RoEO-PLGA _B gel formulations were tested for the behavior of the gel during increasing shear rate (ramp-up, blue line) and decreasing shear rate (rampdown, red line). This type of test was performed to assess whether the two formulations exhibit thixotropy or hysteresis in their flow behavior (Table 3).

Table 3. Comparative analysis of rheological properties of RoEO-PLGA systems.

Parameter	RoEO-PLGA _A (35 ◦C)	RoEO-PLGA _B (36.6 ◦C)	Comment
Hysteresis loop area (Pa/s)	12.02	−168.50	positive/negative value indicates a thixotropic/ rheotropic liquid
Thixotropic index (TI) (RPM1/RPM2 = 1/10)	9.48	6.86	TI > 1: shear thinning TI = 1: Newtonian liquid TI < 1: shear thickening
Energy dissipation ratio (%)	13.94	−8.34	negative value indicates the rheopectic behavior
Shear recovery (%) (shear rate s−1)	76.78	118.86	supra-unitary value is accounted to rheopectic behavior
Yielding stress (Pa)	0.614	14.07	indication of plastic rheology of shear thickening nonNewtonian liquid
Behavior	thixotropic, plastic non-Newtonian liquid	rheopectic, plastic non-Newtonian liquid	RoEO-PLGA_B liquid exhibits, simultaneously, antagonist behavior a plastic rheology and also rheotripsy!

PLGA: Poly(lactic-co-glycolic) acid; RoEO: Rosemary essential oil; RPM: Revolution per minute.

Table 3 provides a detailed comparative analysis of the rheological properties of two RoEO-PLGA formulations, RoEO-PLGA _A and RoEO-PLGA _B, under specific conditions at 35°C and 36.6°C, respectively. The table includes several key parameters that define the flow and mechanical properties of these thermoresponsive gels. One important parameter is the hysteresis loop area, which reveals the flow behavior of the gels when subjected to shear forces. RoEO-PLGA _A has a positive hysteresis loop area of 12.02 Pa/s, indicating thixotropic behavior, where the gel exhibits shear-thinning properties and breaks down under stress but recovers once the stress is removed. On the other hand, RoEO-PLGA _B shows a negative hysteresis loop area of -168.50 Pa/s, signaling rheopectic behavior, where the gel thickens with shear stress and recovers its structure once the stress is reduced. This duality in behavior highlights that RoEO-PLGA _B exhibits a unique combination of plastic rheology with a rheotropic response, which can be advantageous for specific applications requiring both high viscosity under stress and recovery post-shear. Another critical parameter is the thixotropic index (TI), which further defines the shear behavior of the gels. RoEO-PLGA _A demonstrates a TI of 9.48, which is significantly greater than 1, confirming its shear-thinning nature. This means that the gel becomes less viscous under shear stress, a feature that makes it easier to apply in controlled amounts. RoEO-PLGA _B has a lower TI of 6.86, indicating that it also exhibits shear-thinning properties but to a lesser extent compared to formulation _A. Additionally, the energy dissipation ratio (EDR) for RoEO-PLGA _A is positive (13.94%), suggesting energy loss during the flow, which is typical for thixotropic liquids. Conversely, RoEO-PLGA _B has a negative EDR (-8.34%), reinforcing its rheopectic nature where energy is stored during shear and released once the stress is removed. The shear recovery percentage, which indicates the gel's ability to return to its original structure after shear, is 76.78% for RoEO-PLGA _A and 118.86% for RoEO-PLGA _B, showing that formulation _B exhibits superior recovery, contributing to its rheopectic behavior. The yielding stress, which defines the stress required to initiate flow in a material, is lower in RoEO-PLGA _A (0.614 Pa) compared to RoEO-PLGA _B (14.07 Pa). This suggests that RoEO-PLGA _A is more fluid and easier to deform under minimal stress, while RoEO-PLGA _B behaves more like a plastic material, requiring higher stress to begin flow. Overall, the rheological data indicates that RoEO-PLGA _A is a thixotropic, plastic, non-Newtonian liquid, suitable for applications requiring shear-thinning and easy application, while RoEO-PLGA _B displays a combination of plastic rheology and rheotropic behavior, making it more resilient under stress with enhanced recovery. These differing behaviors suggest that both formulations offer unique benefits depending on the desired application, with RoEO-PLGA _A being ideal for situations requiring smooth, easy flow and RoEO-PLGA _B for more robust, stress-resistant uses.

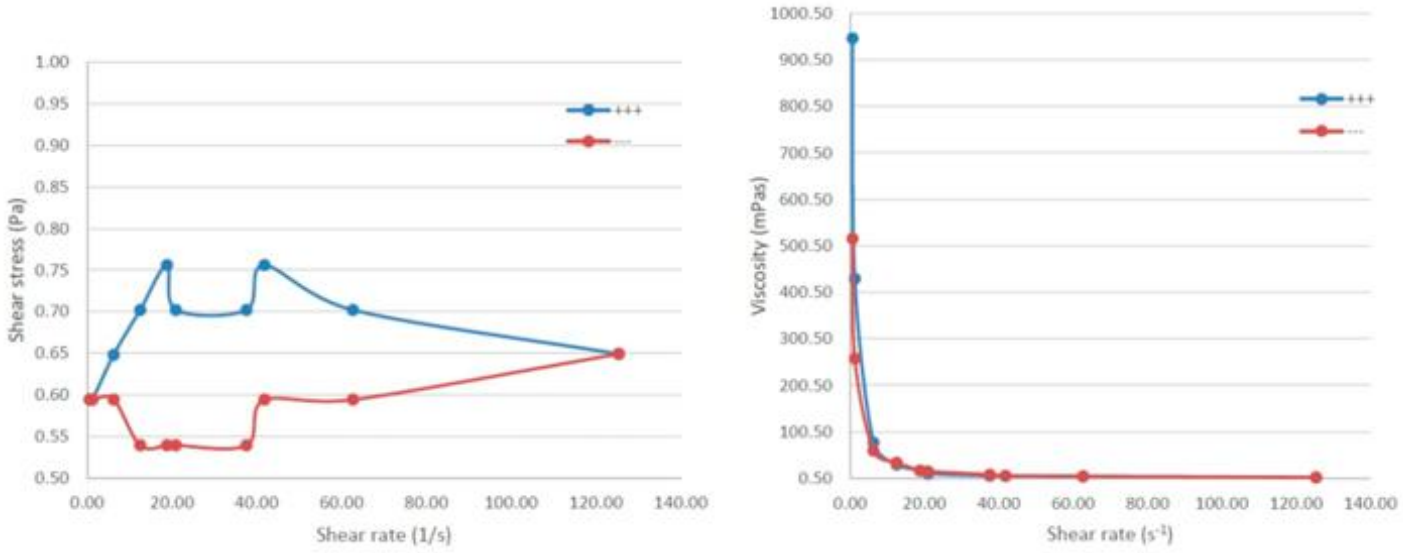

Figure 10. Rheological behavior of RoEO-PLGA _A: (a) Relationship between shear stress and shear rate (blue—increasing shear rate; red—decreasing shear rate); (b) Viscosity under varying shear rates (at 36 ◦C; blue—increasing shear rate; red—decreasing shear rate).

Figure 10 illustrates the rheological behavior of RoEO-PLGA _A, showcasing two distinct aspects of its response to varying shear rates. Panel (a) demonstrates the relationship between shear stress (in Pa) and shear rate (in 1/s) for the formulation, with two lines representing the increasing (blue) and decreasing (red) shear rates. The graph reveals the typical shear-thinning behavior of RoEO-PLGA _A, where the shear stress initially increases with shear rate up to a certain point, after which it sharply decreases as the shear rate is further increased. This indicates that the material becomes less resistant to deformation as the shear rate rises. Interestingly, the graph also shows a slight increase in shear stress during the decreasing shear rate phase, which is a hallmark of thixotropic behavior. The formulation thus exhibits time-dependent shear-thinning properties, where it temporarily loses its structure under stress but recovers as the stress is reduced.

Panel (b) presents the viscosity data under varying shear rates, where the viscosity (in mPa.s) is plotted against the shear rate. As expected for a shear-thinning material, the viscosity decreases significantly as the shear rate increases. The viscosity of the RoEO-PLGA _A formulation starts high at low shear rates, suggesting that the gel is quite thick and resistant to flow under low shear conditions. However, as the shear rate increases, the viscosity drops rapidly, leveling off at much lower values, which is indicative of the material's ability to flow more easily under higher shear. The red line, representing the decreasing shear rate, shows a similar trend but with a slightly higher viscosity at higher shear rates, further demonstrating the formulation's thixotropic nature. This rheological profile underscores the formulation's potential for applications requiring shear thinning, such as topical drug delivery systems, where the material can flow easily upon application but quickly regain its structure once the stress is removed.

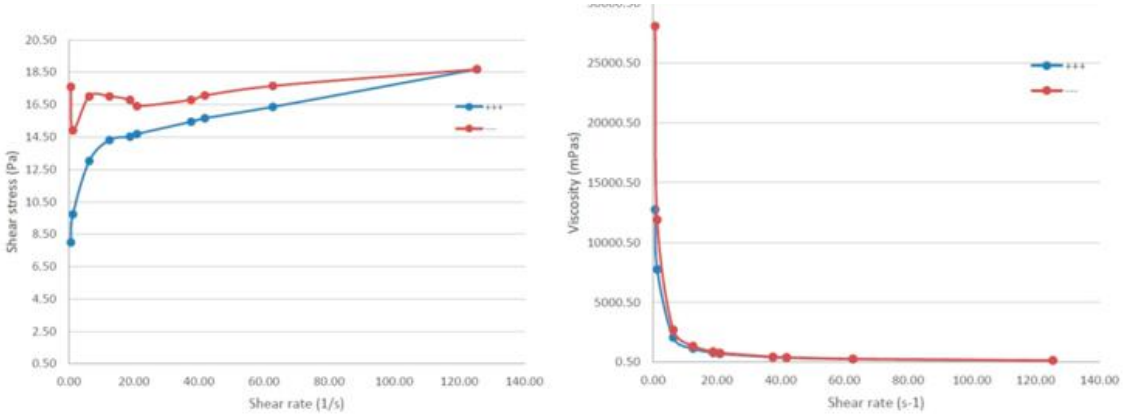

Figure 11. Rheological behavior of RoEO-PLGA _B: (a) Relationship between shear stress and shear rate (blue—increasing shear rate; red—decreasing shear rate); (b) Viscosity under varying shear rates (at 36 ◦C; blue—increasing shear rate; red—decreasing shear rate).

Figure 11 illustrates the rheological behavior of RoEO-PLGA _B, detailing its response to varying shear rates. Panel (a) shows the relationship between shear stress (in Pa) and shear rate (in 1/s), with the blue line representing the increasing shear rate and the red line showing the decreasing shear rate. The graph reveals a distinct behavior where the shear stress increases gradually as the shear rate rises, reaching a plateau at higher shear rates. This indicates that the formulation behaves in a rheopectic manner, meaning it exhibits

an increase in viscosity and shear stress as shear rate is applied and then maintained once the shear rate is removed. The formulation thus becomes more resistant to deformation at higher shear rates, a characteristic that is opposite to the shear-thinning behavior seen in thixotropic materials. The red line (decreasing shear rate) shows that the shear stress slightly remains elevated compared to the increasing shear rate phase, further supporting the rheopectic behavior. Panel (b) presents the viscosity data (in mPa.s) under varying shear rates, where viscosity decreases sharply with increasing shear rate. The viscosity remains high at low shear rates, suggesting that the formulation has a strong resistance to flow. As the shear rate increases, the viscosity drops rapidly, leveling off as the shear rate exceeds certain values. The red curve (decreasing shear rate) shows similar behavior but with a slight increase in viscosity, highlighting the rheopectic characteristics of the formulation. RoEO-PLGA _B thus behaves as a shear-thickening material, where its internal structure builds up with shear stress, increasing the resistance to flow at higher shear rates. This rheological profile makes the formulation suitable for applications where increased viscosity at higher shear rates is required, such as in controlled-release drug delivery systems or coatings.

3.8 Antimicrobial Activity

We used the agar well diffusion method to evaluate the antibacterial properties of RoEO, RoEO Tunisia reference, RoEO-PLGA _A, and RoEO-PLGA _B in vitro. One Gram-positive (Staphylococcus aureus), one Gram-negative (Escherichia coli), and one fungal (Candida albicans) organism was the focus of this evaluation. Table 4 displays the results. Inhibition zones (IZs) observed against all tested microbes ranged from 9.9 mm to 27.2 mm.

Table 4. Average diameters of bacterial growth inhibition zones.

Tested Microorganism	Diameter of Inhibition Area (mm)					
	1	2	3	4	5	6
S. aureus	14.5	14.5	12.7	12.8	0	0
E. coli	10.7	11.6	9.8	11.7	0	0
C. albicans	10.8	12.8	27.0	27.2	0	0

1: RoEO Tunisia reference; 2: RoEO; 3: RoEO-PLGA _A; 4: RoEO-PLGA _B; 5, 6: Negative controls (sterile saline solution and sterile distilled water, respectively); PLGA: Poly(lactic-co-glycolic) acid; RoEO: Rosemary essential oil.

The most significant inhibitory activity was observed against C. albicans, highlighting its enhanced susceptibility to the formulations. Interestingly, the RoEO sample exhibited slightly larger IZs than the RoEO Tunisia reference, emphasizing potential differences in composition or activity (Figure 12a–c).

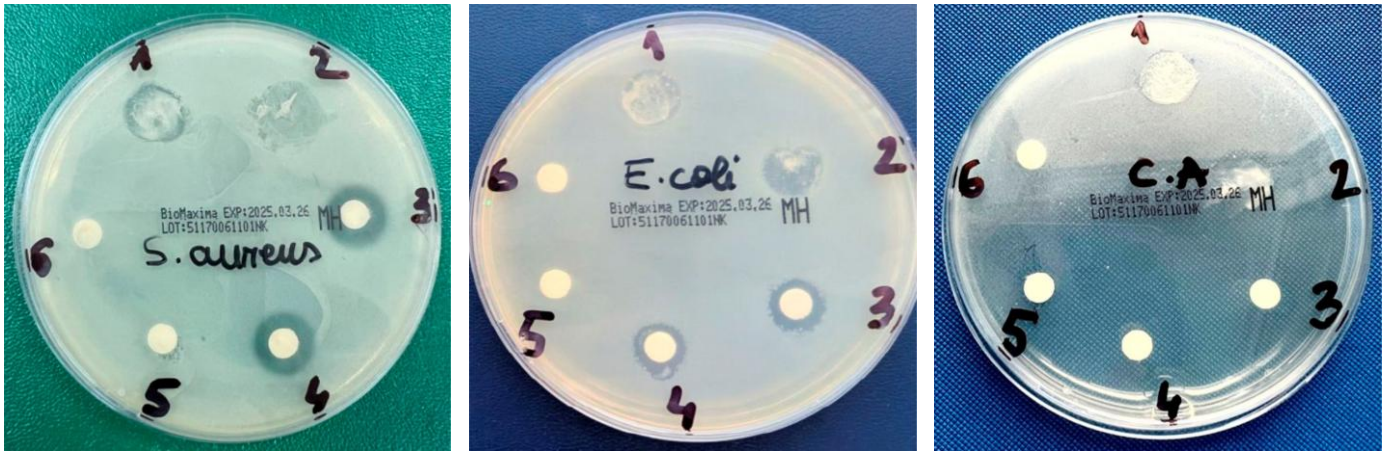

Figure 12. Antimicrobial screening against (a) S. aureus, (b) E. coli, and (c) a fungal strain (C. albicans).

The inhibition zones measure the antibacterial effectiveness, which is dependent on how fast the active chemicals diffuse through the agar medium. Due to the controlled release mechanism, the enclosed RoEO in PLGA microparticles is expected to diffuse more slowly than free RoEO. The observation of somewhat smaller inhibitory zones for S. aureus and E. coli in the RoEO-PLGA gels compared to pure RoEO may be explained by this phenomena. On the other hand, pure RoEO had a narrower inhibition zone for Candida albicans (10.8-12.8 mm), whereas RoEO-PLGA gels had a much wider zone (27.0-27.2 mm), suggesting that the antifungal efficacy is enhanced by the prolonged release of bioactive substances, which maintains a potent concentration across a wider region. Depending on the formulation's release kinetics, the amounts of active substances near the diffusion area border may change. The longer the release of bioactive chemicals, the more uniform their concentration is across a larger area, which explains why RoEO-PLGA gels result in larger inhibitory zones for Candida albicans (27.0-27.2 mm) compared to pure RoEO (10.8-12.8 mm). A controlled release mechanism is enabled by RoEO integration into PLGA microparticles, which likely significantly contributes to the enhancement of antifungal activity against Candida albicans. For some bacterial strains, including S. aureus and E. coli, the controlled release mechanism may not be as important since the active chemicals need to be accessible quickly. Also, changes in how susceptible microbial cell

membranes are to the active compounds might account for the observed differences. The Gram-positive bacteria's signature strong cellular architecture The outer layer of Gram-negative bacteria, Staphylococcus aureus, and Antimicrobial drug distribution and efficacy may be impacted by E. coli in a way different from that of fungal organisms.

4. Discussion

A major step forward in controlled drug delivery and antimicrobial therapy has been achieved with the invention of biocompatible thermoresponsive gels enhanced with poly(lactic-co-glycolic) acid (PLGA) microparticles loaded with rosemary essential oil (RoEO). When used together, these materials overcome significant obstacles in contemporary biomedical applications while also capitalising on their unique strengths. One useful technique for drug administration is thermoresponsive gels, which may change from a liquid to a gel when exposed to body temperature [31, 32]. One example of such a gel is one based on poloxamers. The capacity to deliver medications or bioactive chemicals exactly where they are required, without intrusive procedures, is one of the many therapeutic benefits of this temperature-triggered gelation. The therapeutic potential of these systems is further increased by adding essential oils, such as rosemary, which have strong antibacterial and antioxidant characteristics [43, 44].

Based on the significant reduction of bacterial and fungal growth shown in our research, the antimicrobial properties of rosemary essential oil are especially important for wound healing and skin infections. According to research, rosemary can successfully fight off several microbes, including Staphylococcus aureus, Escherichia coli, and Candida albicans, thanks to its abundance of monoterpenes including camphor, α-pinene, and eucalyptol [45, 36]. To address the issues caused by the essential oils' volatility, our analysis found that RoEO incorporated with PLGA microparticles showed regulated release. Important for maintaining antimicrobial efficacy for an extended period of time, this encapsulating technique keeps the therapeutic chemicals stable and allows for continuous release over time [47, 58]. The controlled release method greatly improves antifungal activity, since the RoEO-PLGA formulations showed a wider inhibition zone against C. albicans than free RoEO. Essential oils are naturally unstable and degrade quickly when exposed to external influences; however, encasing RoEO in PLGA microparticles helps overcome this. PLGA, a biodegradable and biocompatible polymer, has the capacity to encapsulate a variety of bioactive compounds, stabilising them and allowing for guided continuous release [9, 10]. Substances that are hydrophobic and volatile, such as essential oils, may be reliably and consistently delivered using PLGA, which has been the subject of much research into its use in drug delivery systems [21, 62]. Dynamic light scattering (DLS) examination indicated that the oil-in-water emulsion approach effectively contained RoEO in PLGA microparticles, leading to homogenous microparticles with a size distribution of around 1.98 µm, which were the focus of the present work. The microparticles stay stable and distribute well inside the gel formulation because of this constant particle size, which adds to the drug delivery system's dependability and homogeneity [63, 64].

The gel compositions' thermoresponsiveness, together with their antibacterial capabilities, makes them highly useful, especially for transdermal and topical medication administration. The gels are engineered to stay liquid at lower temperatures and solidify when they reach the skin's physiological temperature, offering a simple and painless way to administer drugs. Thanks to this phase transition, the gel sticks firmly to the skin when applied, creating a solid layer that gradually releases the active components as it becomes warmed up by the body. Because of this quality, the gel formulation is very suitable for use in wound healing applications, as it can transport antibacterial and therapeutic chemicals to the infection site without requiring constant reapplication [45, 27]. Further validation of the gel compositions' appropriateness for practical usage was provided by rheological investigations. The gels' shear stress behaviour and viscosity were assessed using a battery of dynamic experiments, which included ramp-up and ramp-down shear rates. These materials are characterised by a time-dependent reduction in viscosity under shear stress [17], and the findings showed that both formulations displayed non-Newtonian, thixotropic behaviour. Because of their thixotropic properties, gel formulations may be applied to the skin with ease and swiftly return to their gel structure when the shear force is eliminated. There was a stronger gel structure in the formulation that had a higher concentration of Poloxamer 407. This was shown by a higher thixotropic index and a more noticeable yield stress. The gel's rheological characteristics make it stick to the skin after application and provide sustained, efficient delivery of the encapsulated RoEO.

The RoEO-PLGA formulation exhibited good thermal stability according to thermogravimetric analysis (TGA) and differential thermogravimetry (DTG). The system remained structurally intact up to about 200°C, after which it degraded significantly, mostly due to the PLGA matrix breaking down. Because the formulation's efficacy depends on its capacity to retain its active components throughout time regardless of storage or application conditions, thermal stability is an important property to have. When developing drug delivery systems that can withstand a wide range of environmental conditions, it is crucial to understand how the formulation reacts to heat [18, 19]. This is where the mass decrease at higher temperatures comes in. The gel compositions' pH values further proved that they were skin-friendly. Because it is in harmony with the skin's natural pH, topical gels work best in the 5–6.5 pH range [20]. The formulations that were evaluated in this research have pH values that fall within this range. This means they are safe for long-term usage in clinical settings and won't irritate the skin. Some bioactive substances are better preserved in slightly acidic environments, hence the gel's pH is an additional factor in the stability of the encapsulated active chemicals. The gel formulation's overall effectiveness and safety are therefore enhanced by this pH range [67].

This study's results show that PLGA thermoresponsive gels infused with rosemary essential oil have great promise as a novel antibacterial and medication delivery system. These formulations show great promise as topical therapies for wound healing, skin infections, and other conditions because to the controlled release of RoEO from PLGA microparticles, the oil's antibacterial activity, and the thermoresponsive gelation capabilities. The gel has the potential to greatly enhance the results of treating many skin problems due to its stability and its capacity to provide prolonged therapeutic concentrations of bioactive chemicals with minimal adverse effects. Improving the gel's mechanical characteristics, optimising the formulation parameters to optimise the release profile, and evaluating its effectiveness in in vivo models of infection and wound healing should be the focus of future investigations. One innovative method for delivering drugs nowadays is to combine essential oils with biodegradable polymers, such as PLGA. The inclusion of rosemary essential oil, which is antibacterial and antioxidant, enhances the therapeutic value of these systems. By working together, these two factors enhance the essential oil's stability and bioavailability while simultaneously laying the groundwork for creative therapeutic solutions. These thermoresponsive gel technologies have the potential to open the door to future medication delivery methods that are both more effective and more patient-friendly with more study and improvement.

5. Conclusions

Thermoresponsive gels loaded with poly(lactic-co-glycolic acid) microparticles containing rosemary essential oil (RoEO) provide a new method for regulated medication delivery and antibacterial treatment, as shown in the research. Overcoming the difficulties of essential oils' volatility and quick degradation, the encapsulation of RoEO in PLGA microparticles guarantees a regulated release of bioactive components. These gels are perfect for topical medication administration because they are thermoresponsive, meaning they change from a liquid to a gel at body temperature. This makes them great for treating skin infections and wounds. The antimicrobial tests showed that the addition of RoEO to the formulation significantly increased the antibacterial effectiveness, particularly against Candida albicans. The gels show great promise as potential clinical applications due to their stability, capacity to provide prolonged therapeutic dosages of bioactive chemicals, and minimal adverse effects. Both gel formulations show thixotropic and non-Newtonian behaviour, according to rheological investigations. This means they are easy to apply and can recover their structure when shear stress is removed. The formulation's compatibility with skin conditions in terms of pH and thermal stability adds to its potential usage in a variety of therapeutic contexts. The benefits of biocompatible, very efficient drug delivery systems that combine essential oils with biodegradable polymers for the treatment of infections and promotion of tissue regeneration are highlighted by the findings of this research. To further improve their therapeutic value, future research should concentrate on optimising these formulations for superior mechanical characteristics, in vivo effectiveness, and release patterns.

References

1. Taylor, M.J.; Tomlins, P.; Sahota, T.S. Thermoresponsive Gels. Gels 2017, 3, 4. [CrossRef] [PubMed]
2. Goponenko, A.V.; Dzenis, Y.A. Role of mechanical factors in applications of stimuli-responsive polymer gels—Status and prospects. Polymer 2016, 101, 415–449. [CrossRef] [PubMed]
3. Pardeshi, S.; Damiri, F.; Zehravi, M.; Joshi, R.; Kapare, H.; Prajapati, M.K.; Munot, N.; Berrada, M.; Giram, P.S.; Rojekar, S.; et al. Functional Thermoresponsive Hydrogel Molecule to Material Design for Biomedical Applications. Polymers 2022, 14, 3126. [CrossRef] [PubMed]
4. Xu, X.; Bizmark, N.; Christie, K.S.S.; Datta, S.S.; Ren, Z.J.; Priestley, R.D. Correction to Thermoresponsive Polymers for Water Treatment and Collection. Macromolecules 2022, 55, 4865. [CrossRef]
5. Bischofberger, I.; Trappe, V. New aspects in the phase behaviour of poly-N-isopropyl acrylamide: Systematic temperature dependent shrinking of PNiPAM assemblies well beyond the LCST. Sci. Rep. 2015, 5, 15520. [CrossRef]
6. Sano, K.; Igarashi, N.; Ebina, Y.; Sasaki, T.; Hikima, T.; Aida, T.; Ishida, Y. A mechanically adaptive hydrogel with a reconfigurable network consisting entirely of inorganic nanosheets and water. Nat. Commun. 2020, 11, 6026. [CrossRef]
7. Klouda, L.; Mikos, A.G. Thermoresponsive hydrogels in biomedical applications. Eur. J. Pharm. Biopharm. 2008, 68, 34–45. [CrossRef]
8. Zarrintaj, P.; Ahmadi, Z.; Saeb, M.R.; Mozafari, M. Poloxamer-based stimuli-responsive biomaterials. Mater. Today Proc. 2018, 5, 15516–15523. [CrossRef]
9. Cui, N.; Dai, C.-Y.; Mao, X.; Lv, X.; Gu, Y.; Lee, E.-S.; Jiang, H.-B.; Sun, Y. Poloxamer-Based Scaffolds for Tissue Engineering Applications: A Review. Gels 2022, 8, 360. [CrossRef]
10. Silva, A.; Costa, A.; Jain, S.; Coelho, E.; Fujiwara, R.; Scher, R.; Nunes, R.; Dolabella, S. Application of Poloxamers for the Development of Drug Delivery System to Treat Leishmaniasis: A Review. Curr. Drug Targets. 2021, 22, 296–309. [CrossRef]
11. Yu, J.; Qiu, H.; Yin, S.; Wang, H.; Li, Y. Polymeric Drug Delivery System Based on Pluronics for Cancer Treatment. Molecules 2021, 26, 3610. [CrossRef] [PubMed]
12. Mayol, L.; Quaglia, F.; Borzacchiello, A.; Ambrosio, L.; La Rotonda, M.I. A novel poloxamers/hyaluronic acid in situ forming hydrogel for drug delivery: Rheological, mucoadhesive and in vitro release properties. Eur. J. Pharm. Biopharm. 2008, 70, 199–206. [CrossRef] [PubMed]

13. Qu, J.; Zhao, X.; Liang, Y.; Zhang, T.; Ma, P.X.; Guo, B. Antibacterial adhesive injectable hydrogels with rapid self-healing, extensibility and compressibility as wound dressing for joints skin wound healing. Biomaterials 2018, 183, 185–199. [CrossRef]
14. [PubMed]
15. de Macedo, L.M.; Santos, É.M.d.; Militão, L.; Tundisi, L.L.; Ataide, J.A.; Souto, E.B.; Mazzola, P.G. Rosemary (Rosmarinus officinalis L., syn Salvia rosmarinus Spenn.) and Its Topical Applications: A Review. Plants 2020, 9, 651. [CrossRef]
16. Raškovic´, A.; Milanovic´, I.; Pavlovic´, N.; Cebovic´, T.; Vukmirovic´, S.; Mikov, M. Antioxidant activity of rosemary (´ Rosmarinus officinalis L.) essential oil and its hepatoprotective potential. BMC Complement. Altern. Med. 2014, 14, 225. [CrossRef]
17. Veenstra, J.P.; Johnson, J.J. Rosemary (Salvia rosmarinus): Health-promoting benefits and food preservative properties. Int. J.
18. Nutr. 2021, 6, 1–10. Available online: https://pmc.ncbi.nlm.nih.gov/articles/PMC8513767/ (accessed on 12 November 2024). [CrossRef]
19. al-Sereiti, M.R.; Abu-Amer, K.M.; Sen, P. Pharmacology of rosemary (Rosmarinus officinalis Linn.) and its therapeutic potentials. Indian
20. J. Exp. Biol. 1999, 37, 124–130. Available online: https://www.bioline.org.br/request?ie99026 (accessed on 12 November 2024).
21. Bejenaru, L.E.; Bi¸tă, A.; Mogos¸anu, G.D.; Segneanu, A.-E.; Radu, A.; Ciocîlteu, M.V.; Bejenaru, C. Polyphenols Investigation and Antioxidant and Anticholinesterase Activities of Rosmarinus officinalis L. Species from Southwest Romania Flora. Molecules 2024, 29, 4438. [CrossRef]
22. de Oliveira, J.R.; de Jesus, D.; Figueira, L.W.; de Oliveira, F.E.; Pacheco Soares, C.; Camargo, S.E.A.; Jorge, A.O.C.; de Oliveira, L.D.
23. Biological activities of Rosmarinus officinalis L. (rosemary) extract as analyzed in microorganisms and cells. Exp. Biol. Med. 2017,
24. 242, 625–634. [CrossRef]
25. Wang, W.; Li, N.; Luo, M.; Zu, Y.; Efferth, T. Antibacterial Activity and Anticancer Activity of Rosmarinus officinalis L. Essential Oil Compared to That of Its Main Components. Molecules 2012, 17, 2704–2713. [CrossRef]
26. González-Vallinas, M.; Molina, S.; Vicente, G.; Zarza, V.; Martín-Hernández, R.; García-Risco, M.R.; Fornari, T.; Reglero, G.;
27. Ramírez de Molina, A. Expression of MicroRNA-15b and the Glycosyltransferase GCNT3 Correlates with Antitumor Efficacy of
28. Rosemary Diterpenes in Colon and Pancreatic Cancer. PLoS ONE 2014, 9, e98556. [CrossRef] [PubMed]
29. Yu, M.H.; Choi, J.H.; Chae, I.G.; Im, H.G.; Yang, S.A.; More, K.; Lee, I.S.; Lee, J. Suppression of LPS-induced inflammatory activities by Rosmarinus officinalis L. Food Chem. 2013, 136, 1047–1054. [CrossRef]
30. Al-Megrin, W.A.; AlSadhan, N.A.; Metwally, D.M.; Al-Talhi, R.A.; El-Khadragy, M.F.; Abdel-Hafez, L.J.M. Potential antiviral agents of Rosmarinus officinalis extract against herpes viruses 1 and 2. Biosci. Rep. 2020, 40, BSR20200992. [CrossRef] [PubMed]
31. Ghasemzadeh Rahbardar, M.; Hosseinzadeh, H. Therapeutic effects of rosemary (Rosmarinus officinalis L.) and its active constituents on nervous system disorders. Iran J. Basic Med. Sci. 2020, 23, 1100–1112. [CrossRef] [PubMed]
32. Borges, R.S.; Ortiz, B.L.S.; Pereira, A.C.M.; Keita, H.; Carvalho, J.C.T. Rosmarinus officinalis essential oil: A review of its phytochemistry, anti-inflammatory activity, and mechanisms of action involved. J. Ethnopharmacol. 2019, 229, 29–45. [CrossRef]
33. Sienkiewicz, M.; Łysakowska, M.; Pastuszka, M.; Bienias, W.; Kowalczyk, E. The Potential of Use Basil and Rosemary Essential Oils as Effective Antibacterial Agents. Molecules 2013, 18, 9334–9351. [CrossRef]
34. Jiang, Y.; Wu, N.; Fu, Y.J.; Wang, W.; Luo, M.; Zhao, C.J.; Zu, Y.G.; Liu, X.L. Chemical composition and antimicrobial activity of the essential oil of Rosemary. Environ. Toxicol. Pharmacol. 2011, 32, 63–68. [CrossRef]
35. Brizuela Guerra, N.; Correa Ferrán, D.; Caldas de Sousa, V.; Delgado García-Menocal, J.A.; García Vallés, M.; Martínez, S.; Morejón Alonso, L.; Loureiro dos Santos, L.A. Development of poly (lactic-co-glycolic acid)/bioglass fibers using an electrospinning technique. Lat. Am. Appl. Res. 2018, 48, 131–138. [CrossRef]
36. Khanal, S.; Adhikari, U.; Rijal, N.P.; Bhattarai, S.R.; Sankar, J.; Bhattarai, N. pH-Responsive PLGA Nanoparticle for Controlled Payload Delivery of Diclofenac Sodium. J. Funct. Biomater. 2016, 7, 21. [CrossRef]

37. Segneanu, A.-E.; Vlase, G.; Vlase, T.; Bejenaru, L.E.; Mogos¸anu, G.D.; Buema, G.; Herea, D.-D.; Ciocîlteu, M.V.; Bejenaru, C. Insight into Romanian Wild-Grown Heracleum sphondylium: Development of a New Phytocarrier Based on Silver Nanoparticles with Antioxidant, Antimicrobial and Cytotoxicity Potential. Antibiotics 2024, 13, 911. [CrossRef]
38. Aina, A.; Gupta, M.; Boukari, Y.; Morris, A.; Billa, N.; Doughty, S. Monitoring model drug microencapsulation in PLGA scaffolds using X-ray powder diffraction. Saudi Pharm. J. 2016, 24, 227–231. [CrossRef] [PubMed]
39. Amani, F.; Sami, M.; Rezaei, A. Characterization and Antibacterial Activity of Encapsulated Rosemary Essential Oil within Amylose Nanostructures as a Natural Antimicrobial in Food Applications. Starch Stärke 2021, 73, 2100021. [CrossRef]
40. Lagreca, E.; Onesto, V.; Di Natale, C.; La Manna, S.; Netti, P.A.; Vecchione, R. Recent advances in the formulation of PLGA microparticles for controlled drug delivery. Prog. Biomater. 2020, 9, 153–174. [CrossRef] [PubMed]
41. Micic´, D.; Đurovic´, S.; Riabov, P.; Tomic´, A.; Šovljanski, O.; Filip, S.; Tosti, T.; Dojc˘inovic´, B.; Božovic´, R.; Jovanovic´, D.; et al. Rosemary Essential Oils as a Promising Source of Bioactive Compounds: Chemical Composition, Thermal Properties, Biological Activity, and Gastronomical Perspectives. Foods 2021, 10, 2734. [CrossRef]
42. Wang, J.; Liu, L.; Zhang, S.; Liao, B.; Zhao, K.; Li, Y.; Xu, J.; Chen, L. Review of the Perspectives and Study of Thermo-Responsive Polymer Gels and Applications in Oil-Based Drilling Fluids. Gels 2023, 9, 969. [CrossRef]
43. Matanovic´, M.R.; Kristl, J.; Grabnar, P.A. Thermoresponsive polymers: Insights into decisive hydrogel characteristics, mechanisms of gelation, and promising biomedical applications. Int. J. Pharm. 2014, 472, 262–275. [CrossRef]
44. Lambers, H.; Piessens, S.; Bloem, A.; Pronk, H.; Finkel, P. Natural skin surface pH is on average below 5, which is beneficial for its resident flora. Int. J. Cosmet. Sci. 2006, 28, 359–370. [CrossRef]
45. Matsumoto, K.; Sakikawa, N.; Miyata, T. Thermo-responsive gels that absorb moisture and ooze water. Nat. Commun. 2018, 9, 2315. [CrossRef]
46. Qi, X.; Xiang, Y.; Li, Y.; Wang, J.; Chen, Y.; Lan, Y.; Liu, J.; Shen, J. An ATP-activated spatiotemporally controlled hydrogel prodrug system for treating multidrug-resistant bacteria-infected pressure ulcers. Bioact. Mater. 2024, 45, 301. [CrossRef]
47. Qi, X.; Cai, E.; Xiang, Y.; Zhang, C.; Ge, X.; Wang, J.; Lan, Y.; Xu, H.; Hu, R.; Shen, J. An Immunomodulatory Hydrogel by
48. Hyperthermia-Assisted Self-Cascade Glucose Depletion and ROS Scavenging for Diabetic Foot Ulcer Wound Therapeutics. Adv. Mater. 2023, 35, 2306632. [CrossRef]
49. Chen, Y.; Sha, X.; Zhang, W.; Zhong, W.; Fan, Z.; Ren, Q.; Chen, L.; Fang, X. Pluronic mixed micelles overcoming methotrexate multidrug resistance: In vitro and in vivo evaluation. Int. J. Nanomed. 2013, 8, 1463–1476. [CrossRef]
50. Higuchi, A.; Aoki, N.; Yamamoto, T.; Gomei, Y.; Egashira, S.; Matsuoka, Y.; Miyazaki, T.; Fukushima, H.; Jyujyoji, S.; Natori, S.H. Bioinert Surface of Pluronic-Immobilized Flask for Preservation of Hematopoietic Stem Cells. Biomacromolecules 2006, 7, 1083–1089. [CrossRef] [PubMed]
51. Santander-Ortega, M.J.; Csaba, N.; Alonso, M.J.; Ortega-Vinuesa, J.L.; Bastos-González, D. Stability and physicochemical characteristics of PLGA, PLGA:poloxamer and PLGA:poloxamine blend nanoparticles: A comparative study. Colloids Surf. A
52. Physicochem. Eng. Asp. 2007, 296, 132–140. [CrossRef]
53. Hamoudi-Ben Yelles, M.C.; Tran Tan, V.; Danede, F.; Willart, J.F.; Siepmann, J. PLGA implants: How Poloxamer/PEO addition slows down or accelerates polymer degradation and drug release. J. Control. Release 2017, 253, 19–29. [CrossRef]
54. Borges, M.F.d.A.; Lacerda, R.d.S.; Correia, J.P.d.A.; de Melo, T.R.; Ferreira, S.B. Potential Antibacterial Action of α-Pinene. Med. Sci. Forum 2022, 12, 11. [CrossRef]
55. Duda-Madej, A.; Viscardi, S.; Grabarczyk, M.; Topola, E.; Kozłowska, J.; Ma¸czka, W.; Win´ska, K. Is Camphor the Future in Supporting Therapy for Skin Infections? Pharmaceuticals 2024, 17, 715. [CrossRef]
56. Elangovan, S.; Mudgil, P. Antibacterial Properties of Eucalyptus globulus Essential Oil against MRSA: A Systematic Review. Antibiotics 2023, 12, 474. [CrossRef]
57. Salehi, B.; Upadhyay, S.; Erdogan Orhan, I.; Kumar Jugran, A.; Jayaweera, S.L.D.; Dias, D.A.; Sharopov, F.; Taheri, Y.; Martins, N.; Baghalpour, N.; et al. Therapeutic Potential of α- and β-Pinene: A Miracle Gift of Nature. Biomolecules 2019, 9, 738. [CrossRef]
58. Xie, Z.; Zheng, Z.; Chen, C.; Li, G.; Wang, X. Borneol-Modified Chitosan Coating with Antibacterial Properties via Layer-by-Layer Strategy. Coatings 2024, 14, 381. [CrossRef]
59. Cordeiro, L.; Figueiredo, P.; Souza, H.; Sousa, A.; Andrade-Júnior, F.; Medeiros, D.; Nóbrega, J.; Silva, D.; Martins, E.; BarbosaFilho, J.; et al. Terpinen-4-ol as an Antibacterial and Antibiofilm Agent against Staphylococcus aureus. Int. J. Mol. Sci. 2020, 21, 4531. [CrossRef]
60. Su, R.; Guo, P.; Zhang, Z.; Wang, J.; Guo, X.; Guo, D.; Wang, Y.; Lü, X.; Shi, C. Antibacterial Activity and Mechanism of Linalool against Shigella sonnei and Its Application in Lettuce. Foods 2022, 11, 3160. [CrossRef] [PubMed]

61. Khedhri, S.; Polito, F.; Caputo, L.; De Feo, V.; Khamassi, M.; Kochti, O.; Hamrouni, L.; Mabrouk, Y.; Nazzaro, F.; Fratianni, F.; et al. Chemical Composition, Antibacterial Properties, and Anti-Enzymatic Effects of Eucalyptus Essential Oils Sourced from Tunisia. Molecules 2023, 28, 7211. [CrossRef] [PubMed]
62. Ma, Y.; Cong, Z.; Gao, P.; Wang, Y. Nanosuspensions technology as a master key for nature products drug delivery and In vivo fate. Eur. J. Pharm. Sci. 2023, 185, 106425. [CrossRef]
63. Linz, M.S.; Mattappallil, A.; Finkel, D.; Parker, D. Clinical Impact of Staphylococcus aureus Skin and Soft Tissue Infections. Antibiotics 2023, 12, 557. [CrossRef] [PubMed]
64. Mariani, F.; Galvan, E.M. Staphylococcus aureus in Polymicrobial Skin and Soft Tissue Infections: Impact of Inter-Species Interactions in Disease Outcome. Antibiotics 2023, 12, 1164. [CrossRef] [PubMed]
65. Kashem, S.W.; Kaplan, D.H. Skin Immunity to Candida albicans. Trends Immunol. 2016, 37, 440–450. [CrossRef]
66. Loftsson, T.; Masson, M. Cyclodextrins in topical drug formulations: Theory and practice. Int. J. Pharm. 2001, 225, 15–30. [CrossRef]
67. Rău, G.; Cre¸tu, F.M.; Andrei, A.M.; Pisoschi, C.G.; Mogos¸anu, G.D.; Boroghină, A.; Bani¸tă, I.M.; Stănciulescu, C.E. Synthesis and evaluation of antimicrobial activity of new 2-mercapto-3-substituted-1,4-naphthoquinones (I). Farmacia 2015, 63, 665–669. Available online: https://farmaciajournal.com/wp-content/uploads/2015-05-art-07-Rau_Pisoschi_665-669.pdf (accessed on 18 November 2024).

*****